Research Square

Preprints are preliminary reports that have not undergone peer review.
They should not be considered conclusive, used to inform clinical practice,
or referenced by the media as validated information.

Targeting Hedgehog pathway and DNA methyltransferases suppress the phenotype of uterine leiomyosarcoma cells

Natalia Garcia
University of Illinois at Chicago College of Medicine
Ayman Al-Hendy
University of Illinois at Chicago College of Medicine
Edmund Chada Baracat
Universidade de Sao Paulo
Katia Candido Carvalho
Universidade de Sao Paulo
Qiwei Yang (qiwei@uic.edu)
University of Illinois at Chicago College of Medicine https://orcid.org/0000-0001-7131-8946

Research article

Keywords: Uterine leiomyosarcoma, Hedgehog signaling, Inhibitor

Posted Date: May 27th, 2020

DOI: https://doi.org/10.21203/rs.3.rs-27677/v1

License: This work is licensed under a Creative Commons Attribution 4.0 International License.
Read Full License

Abstract

Background: Uterine leiomyosarcoma (LMS) is an aggressive tumor with poor prognosis, high rates of recurrence and metastasis. Several studies have shown an essential role of Hedgehog (HH) signaling in tumor development. The role of HH pathway in LMS is still unclear.

Methods: Uterine smooth muscle (USTM) and LMS cells lines were used to evaluate the mRNA and protein expression of HH components. MTT assay was performed to evaluate the inhibitory effect of SMO, GLI1 and DNMT inhibitors for proliferation. Nuclear and cytoplasm fractions were prepared. Protein and RNA expression levels were determined by Western blot and q-PCR analysis. Migration, invasion and apoptosis assays were performed to determine the LMS phenotype after the treatments. The statistical analysis was performed using GraphPad Prism 5, and the statistical significance was accepted for $p<0.05$.

Results: LMS analyses showed upregulation of SMO and GLIs (1, 2 and 3) in LMS compared to the myometrium and uterine leiomyoma. Increased nuclear translocation of GLIs proteins was found in LMS cells as well. After that, we hypothesized that HH pathway could be activated in uterine LMS and its blocking would lead to LMS malignant phenotype suppression. Inhibition of SMO and GLI after treatment with LDE225 and Gant61 respectively, induced both protein downregulation as well as decreased GLIs nuclear translocation. Also, abnormal increased expression of DNMT (1, 3a, and 3b) was observed in LMS, and treatment with a DNMT inhibitor decreased both DNMTs expression and GL1 nuclear translocation.

Conclusion: Our analyses showed that deactivation of SMO, GLI and DNMTs was able to inhibit LMS phenotype. Importantly, the combination of those treatments exhibited a potentiated effect on LMS malignant phenotype suppression, leading to a deactivating HH pathway. In conclusion, our studies may provide novel options for uterine LMS patients´ target therapy.

Background

Uterine leiomyosarcoma (LMS) is a rare uterine cancer, representing 1–2% of all uterine malignancies (1). The annual incidence of LMS is approximately 0.8 per 100,000 women (2). The 5 years survival for all patients to be between 25 and 76%, with survival for women with metastatic disease at the time of initial diagnosis approaching only 10–15% (3). Irrespective of treatment, the LMS is characterized by poor prognosis (4), LMS patients' present treatment resistance to currently available therapies as evidenced by high rates of both recurrence and progression (5).

The first evidence of Hedgehoh (HH) pathway deregulation in LMS patients was described by Garcia and collaborators (6). Higher protein expression levels of SMO and GLI1 were found in LMS samples compared to myometrium and leiomyoma variants. Additionally, increased expression of SHH and SUFU were correlated with decreased overall survival (6).

The HH signaling pathway plays an essential role in several biological processes, including embryonic development, tissue differentiation, as well as the pathogenesis of multiple cancer types (6–9). Activation of the canonical HH signaling pathway occurs when HH ligand binds and inactivates PTCH1, releasing SMO protein signaling to its cytoplasm targets (10). SMO is a G protein-coupled receptor-like (GPCR-like) protein, which triggers GLI proteins translocation to the nucleus and its consequent binding to DNA (11). GLI1 has only an activator form, while GLI2 and GLI3 have both activator (GLI2A and GLI3A) and repressor forms (GLI2R and GLI3R) (12). GLI members act as the nuclear effectors at the end of the pathway, which is responsible for regulating the expression of downstream target genes (13).

HH signaling pathway activation can also occur due to epigenetic mechanisms. It has been observed that the promoter region in HH ligand is hypomethylated in breast cancer cells (14, 15). GLI3 hypomethylation was observed in gastric cancer (16). Moreover, Hedgehog interacting protein (HHIP) is silenced by promoter hypermethylation in lung and hepatocellular cancers, and this was correlated with downregulation of the protein (17, 18). Hypermethylation at the PTCH1 promoter region has been described in rhabdomyosarcoma, medulloblastomas (19) and breast cancer (20, 21).

PTCH1, as a negative regulatory factor of the HH signaling pathway, could be involved in tumorigenesis. Hypermethylation at *PTCH1* promoter sequences has been observed in astrocytoma and medulloblastoma cell lines contributing to HH signaling activation (22, 23). In addition, alterations in the methylation status of *PTCH1* gene were reported in different types of cancer, suggesting the epigenetic role of *PTCH1* in tumor development (22, 24–26). In this study, we aimed to assess the role and molecular mechanisms of HH pathway activation in LMS and to determine its value as a potential target for anti-LMS therapy.

Methods

Cells and Reagents

The immortalized human leiomyoma cell line (HuLM) and immortalized human uterine smooth muscle (UTSM) cells were a kindly gift from Professor Darlene Dixon. The cells were cultured and maintained in phenol red-free, 10% fetal bovine serum Dulbecco's Modified Eagle Medium: Nutrient Mixture F–12. The leiomyosarcoma (LMS) cell line (SK-UT1, ATCC® HTB–114™) (ATCC, Manassas, VA, USA) was cultured and maintained in ATCC-formulated Eagle's Minimum Essential Medium with 10% of fetal bovine serum.

SMO inhibitors LDE225 and GDC0449 were purchased from Selleck Chemical (Houston TX, USA), GLI inhibitors Gant58 and Gant61 from Sigma Aldrich (St. Louis, MO, USA) and DNA methylation inhibitor 5' Aza- 2'-deoxycytidine from Biosynth & Carbosynth (Staad, St. Gallen, Switzerland).

Proliferation assay

Cell proliferation was measured using dimethythiazoldiphenyltetra-zoliumbromide (MTT Sigma Aldrich, St. Louis, MO, USA) assay. 2x10³ cells per well were seeded into 96-well tissue culture plates, treated as described in the figure legends and MTT assay was performed at different time points (24, 48, 72 and 96h). Absorbance was measured in a synergy HT multi-detection microplate reader (BioTek, Broadview, Illinois, USA) at 570 nm. This assay was performed three times in triplicate

Cell treatment using Hedgehog pathway and DNA methyltransferase inhibitors

LMS cells were seeded at $8x10^4$ per well in a six-well plate and cultured overnight, then LMS cells were treated with SMO- LDE225 (10 μM), GLI-Gant61 (30 μM) or DNMT- 5'-Aza-dc (2 μM) inhibitors for 72 hours, with daily replacement/change. After the treatment, the cells were harvested for protein/RNA expression measurement,and other studies. The experiments were performed three times in triplicate.

RNA extraction and gene expression

Total RNA was isolated using Trizol reagent (Invitrogen, California USA). The concentration of total RNA was determined using NanoDrop (Thermo Scientific, Waltham, MA). One microgram of total RNA from each sample was reverse-transcribed to complementary DNA (cDNA) using the High Capacity cDNA Transcription Kit (Thermo Scientific, Waltham, MA). Quantitative real-time polymerase chain reaction (qRT-PCR) was performed to determine the messenger RNA (mRNA) expression of several genes listed with their primer sequences in Table S1, all primers were selected from literature and the sequences were confirmed using Primer-Blast (https://www.ncbi.nlm.nih.gov/tools/primer-blast/). The real-time PCR reactions were performed using CFX96 PCR instrument using SYBR Green Supermix (Bio-Rad, Hercules, California, USA). *GAPDH, B2M, 18S* and *β-ACTIN* were tested as housekeeping genes and B2M was used as an internal control. The results are presented as relative gene expression using CFX Maestro™. This assay was performed three times in triplicate.

Protein extraction and Western Blot

Cells were collected and lysed in RIPA lysis buffer with protease and phosphatase inhibitor cocktail (Thermo Scientific, Waltham, MA), protein was quantified using the Bradford method (Bio-Rad protein Assay kit). The cytoplasmic and nuclear fractionation was performed using Ner-Per nuclear and cytoplasmic Kit (Thermo Fisher) following the manufacturer's instructions. The information about primary antibodies, including antibody dilution and source of antibodies in this study is listed in Table S2. The antigen-antibody complex was detected with Trident Femto western HRP substrate (GeneTex, Irvine, CA). Specific protein bands were visualized using ChemiDoc XRS þ molecular imager (Bio-Rad).

Migration assay

LMS cells were seeded at 5×10^5 per well in a 24-well plate and cultured overnight. When the cell density reached 100%, a straight scratch was created with a 200 µl pipette tip held perpendicular to the bottom of the 24-well plate (27). The cells were then washed three times with PBS and cultured in serum-free medium with varied treatments. Results were expressed as the space between the edges of individual wounds every 24 hours for 72 hours in comparison with initial (start) time using Image J Software. This assay was performed three-time points in triplicate

Apoptosis Assay

Apoptosis was determined by Annexin V staining (APC Annexin V Apoptosis Detection Kit with 7-AAD, BioLegend, San Diego, California USA) following the manufacturer's instructions. 8×10^3 LMS cells were grown in 6 well plates. The cells were treated with SMO, GLI and DNMT inhibitors for 72 hours. Staurosporine was used as a positive control. The Annexin V stain was evaluated using flow cytometry (Beckman Coulter Gallios).

SMO gene silencing

$5x10^5$ LMS cells were seeded in six-well plates for transfection. Lipofectamine RNAiMAx reagent (Invitrogen, California USA) was used to transfect small interfering RNAs of *SMO* (esiRNA SMO, Sigma Aldrich St. Louis, MO, USA). RNA and protein expression levels were determined at 72 hours post-transfection following the manufacturer's instruction.

PTCH1 Methylation

$8x10^4$ LMS cells were seeded in six-well plates and treated with DNMT inhibitor. The methylation status of *PCTH1* promoter region was determined using the Human cancer EpiTect Methyl II PCR Array® (QIAGEN Sciences, Maryland, USA) following the manufacturer's instructions. The ABI 7500 system for real-time PCR was used to read the plates. The relative amount of methylated and unmethylated DNA was calculated using the standard ΔCt method using an Excel spreadsheet provided by the manufacturer.

Statistical analysis

Comparison of 2 groups was carried out using student *t*-test for parametric distribution and Mann Whitney test for nonparametric distribution. Comparison of multiple groups was carried out by analysis of variance (ANOVA) followed by a post-test using Tukey for parametric distribution and Kruskal-Wallis

test followed by a post-test Dunns for nonparametric distribution, using GraphPad Prism 5 Software. Data were presented as mean ± standard error (SE). The significant difference was defined as $p<0.05$.

Results

Hedgehog is activated in LMS with increased GLI nuclear translocation

The constitutive (basal) expression levels of HH signaling components in UTSM, HuLM, and LMS cells were evaluated by qRT-PCR. Higher expressionof *SMO, SUFU,* and *GLI1* were detected in LMS compared to UTSM ($P<0.05$) and HuLM. The expression of *PTCH1* was down-regulated in LMS. *GLI2* did not show difference among the cells, while *GLI3* was up-regulated in HuLM (Figure 1A). The protein expression levels of SMO and GLI1 were highest in LMS among three detected cell lines. The protein levels of GLI2 and GLI 3 were also upregulated in HuLM. However, SUFU did not show difference among the cell lines (Figure 1B). The expression of HH ligands (*IHH, DHH,* and *SHH)* were not detected in these cells.

We further evaluated the level of GLIs nuclear translocation in UTSM, HuLM and LMS cells (Figure 1C). The expression levels of GLI1 were highest in the nucleus of the LMS cells, low in UTSM and undetected in HuLM cells. GLI2 and GLI3 were mainly expressed in the nucleus of all cell lines, with the highest expression levels in LMS. (Figure 1C). These results showed that HH pathway was activated in LMS due to higher expression of SMO and GLI1 with increased GLI nuclear translocation.

Inhibition of Hedgehog pathway using SMO and GLI inhibitors in LMS cells

SMO inhibitors (LDE225 and GDC0449) and GLI inhibitors (Gant58 and Gant61) were selected to determine their effect on LMS cells. MTT assay was performed using three-time points (24, 48 and 72 h) with varying drug concentrations. Treatment with SMO inhibitor (LDE225) for 72 hours showed a dose-dependent inhibitory effect on cell proliferation (Figure S3 A). 10 μM was used in the following experiments. LMS cells treated with GDC0449 did not show any inhibitory effect using different concentrations (Figure S3 B). GLI1 inhibitor (Gant61) showed a dose-dependent inhibitory effect on LMS after 72 hours of treatment. 30 μM was chosen for the next experiments. While Gant58 did not show an effect on proliferation, Based on MTT results, LDE225 (SMO inhibitor) and Gant61 (GLI inhibitor) were selected for the next experiments (Figure S3 C and D).

To verify the specificity of the effect of SMO (LDE225) and GLI inhibitors (Gant61) on LMS, we performed MTT assay using the same doses and duration in both UTSM and HuLM cells (Figure S4). After 72 hours of treatment, LDE225 and Gant61 showed inhibitory effects on UTSM cells proliferation. SMO inhibitor did not show a significant growth inhibition in UTSM cells (Figure S 4A). While GLI inhibitor showed a significant effect ($p<0.05$) in UTSM (Figure S4 B), however, the proliferation decrease was more potent in

LMS cells when compared with UTSM cells in response to GLi inhibitor. SMO or GLI inhibitors did not show any inhibitory effect on HuLM cells proliferation. These results showed that the HH inhibitors exhibited a dominantly inhibitory effect on LMS. (Figure S4 C and D)

LMS cells were treated with SMO inhibitor, LDE225, for 24, 48 and 72 hours, with drug replacement every 24 hours. RNA and protein expression of HH components were evaluated for all time points. qRT-PCR showed that the expression levels of *SMO, GLI1, GLI2,* and *GLI3* were significantly downregulated after 72 hours LDE225 treatment ($p<0.05$), while alteration of expression levels after 24 and 48 hours treatment was not observed (Figure 2A). The protein expression levels of these key HH members were decreased in a time-dependent manner in response to the treatment of SMO inhibitor (LDE225) (Figure 2B). For GLI inhibitor, qRT-PCR analysis demonstrated that RNA expression of *SMO, GLI1, GLI2,* and *GLI3* was not altered after Gant61 treatment (Figure 2 C). However, protein expression of GLI1, GLI2, and GLI3 were decreased in response to Gant61 treatment (Figure 2D).

The GLIs nuclear translocation was evaluated in LMS cells treated with LDE225 or Gant61 inhibitor for 24, 48, 72 hours, respectively. The results showed that translocation of GLIs into the nucleus was markedly decreased in three-time point treatments with SMO or GLI inhibitor as compared to the untreated control (Figure 2 E and F).

To determine the effects of treatment with LDE225 or Gant61 inhibitor on phenotype of LMS, MTT assay was performed to determine the effect of the treatment on cell proliferation. Our data demonstrated that the proliferation was decreased after treatment with SMO or GLI inhibitor (Figure 2 G and H).

Cell migration is a multi-step process that plays an important role in tumorigenesis. To evaluate the effect of SMO and GLI inhibitors on the migration of LMS cells, would-healing assay was performed. The results showed that the SMO and GLI inhibitor significantly decreased the migration capacity in LMS cells (Figure 3A) ($p<0.05$). Apoptosis assay was performed and demonstrated that SMO and GLI inhibitors induced apoptosis in LMS cells (Figure 3B), the GLI inhibitor showed a more potent effect compared to SMO inhibitor.

To explore the possible synergistic or additive effect of combination treatment with SMO and GLI inhibitors. We evaluated their inhibitory effect on LMS cells using MTT assay. The results showed no synergism or additive effect using a combination of the treatment (Figure S5)

Treatment with SMO or GLI inhibitors individually showed an inhibitory effect on proliferation, migration, and invasion while induced apoptosis in LMS cells. The inhibition of GLI nuclear translocation was more potent using SMO inhibitor. Thus, the SMO gene was selected for knockdown. The knockdown of the SMO gene was performed using interference RNA and the HH components were evaluated in LMS cells. SMO protein expression was evaluated to verify the efficiency of the knockdown and was highly decreased after the knockdown (Figure 3C). Figure 3D shows that knockdown of SMO decreased the expression of SMO, GLI1, GLI2, and GLI3 ($p<0.05$).

Inhibition of DNA methyltransferase regulated HH signaling in LMS cells

To understand the molecular mechanism of activation of the HH signaling pathway in LMS in the context of epigenetic regulation, we determined the expression of DNA methyltransferases (DNMT) in LMS and UTSM cells. Our studies showed that RNA expression of *DNMT1, DNMT3a,* and *DNMT3b* was upregulated in LMS compared to UTSM cells ($p<0.05$) (Figure 4A). Accordingly, the protein expression of DNMT1 and DNMT3a were also increased in the LMS compared to UTSM cells (Figure 4B). Next, we determined whether inhibition of DNA methyltransferases with 5'-Aza–2'-Deoxycytidine (5'-Aza-dc) suppressed LMS phenotype. We performed a MTT assay using a different dose at three-times point (24, 48 and 72 hours). After 72 hours of treatment, 5'-Aza-dc at the concentration of 2 μM showed 50% of inhibition in proliferation (Figure S6 A). PTCH1 DNA methylation was evaluated to verify if the treatment with DNA methyltransferase inhibitor was able to reverse the methylation profile in LMS cells. The basal level of the percentage of PTCH1 DNA methylation in LMS was 2.3%. The percentage of PTCH1 DNA methylation after 72 hours of 5'-Aza-dc treatment was decreased to 1%.

RNA and protein expression levels of DNMTs were evaluated in LMS cells in response to 5'-Aza-dc treatment. The RNA expression of *DNMT1, DNMT3a,* and *DNMT3b* was decreased in 5'-Aza-dc-treated LMS cells compared to the control (Figure 4C). The protein expression of DNMT1 and DNMT3a in LMS cells was also decreased after treatment with 5'-Aza-dc (Figure 4D).

To evaluate the impact of DNA methyltransferase inhibition on the HH signaling pathway, the components of the HH signaling were evaluated in the presence or absence of 5'-Aza-dc in LMS cells. Although the RNA expression of *PTCH1, SMO, SUFU, GLI2,* and *GLI3* was not altered after5'-Aza-dc treatment, the decreased RNA expression of GLI1 was observed in response to 5'-Aza-dc treatment (Figure 5A). WB analysis exhibited decreased expression levels of SMO and GLI1 (Figure 5B). Moreover, GLI1 and GLI2 nuclear translocation were decreased in response to 5'-Aza-dc treatment. On the other hand, 5'-Aza-dc treatment increased the nuclear translocation of GLI3 (Figure 5C).

Next, determine the effect of DNMT inhibition on proliferation, migration, and apoptosis in LMS cells. The results showed that 5'-Aza-dc decreased proliferation (Figure 5D), concomitantly with decreased expression of PCNA proliferation marker in LMS cells (Figure S 6B). Migration capacity was decreased after 5'-Aza-dc treatment ($p<0.05$) (Figure 5E). Moreover, 5'-Aza-dc treatment was capable of inducing apoptosis in LMS cells (Figure 5F).

Inhibition of both DNA Methylation and Hedgehog Signaling in Human LMS cell Lines

The treatment with DNA methyltransferase and HH inhibitors showed an inhibitory effect on HH signaling via decreasing GLI1 transcription and protein expression, as evidenced by decreasing proliferation,

migration and invasion while inducing apoptosis. Next, we performed experiments to explore whether the DNA methyltransferase inhibitor, in combination with HH inhibitors, can exhibit an additive or synergistic effect in LMS cells.

MTT assay was performed to evaluate the combined effect of DNA methylation and HH inhibitors on LMS proliferation. The results showed that the combination treatment with DNA methylation and SMO inhibitors did not show synergism or additive effect. However, the combination of 5'-Aza-dc with GLI inhibitor showed a synergistic effect (Figure S7A). Since the treatment of 1 μM 5'-Aza-dc with 30 μM GLI inhibitor exhibited a most potently inhibitory effect on LMS proliferation, this combination treatment was used for further studies (Figure S7B).

The RNA expression of key HH members including of *SMO, GLI1, GLI2,* and *GLI3* was measured with and without combination treatment, our data demonstrated that combination treatment decreased the RNA expression of *SMO, GLI1, GLI2,* and *GLI3* ($p<0.05$) compared to the control (Figure 6A). The combination treatment also resulted in decreased protein levels of *GLI1* (Figure 6B). Moreover, the combination treatment decreased GLI1 nuclear translocation in a time-dependent manner compared to the control (Figure 6C).

To explore this combination effect on LMS cells phenotype, the cells were treated with both inhibitors for 72 hours, and proliferation was evaluated every 24 hours. Figure 6D showed that combination treatment decreased the proliferation of LMS cells. In addition, the wound-healing assay demonstrated that combination treatment decreased the migration capacity in the LMS cells ($p<0.05$) (Figure 6E). The combination showed a more potent effect comparing to the single treatment, with decrease expression of HH signaling components, proliferation, decreasing GLI1 nuclear translocation and migration capacity in LMS.

Discussion

Uterine leiomyosarcoma is a rare but extremely aggressive tumor that represents a treatment challenge due to its unresponsiveness to available therapies. As a consequence, the patients commonly present high rates of tumor recurrence, progression and metastasis (5).Previously, it was demonstrated thatthe protein levels of SMO and GLI1, the key members of HH signaling, were highly expressed in human uterine LMS (6). However, how HH signaling is activated and its contribution to LMS malignant phenotype are still unknown. In this study, we demonstrated for the first time that HH is activated in LMS cells via upregulation of key HH members concomitantly with increased nuclear translocation of GL1. Importantly, epigenetic mechanisms are involved in the HH pathway activity in LMS cells. Moreover, targeting DNA methylation and HH pathways exhibited a potent inhibitory effect on LMS phenotype.

SMO, GLI, and PTCH1 were selected for evaluation as triggers of the HH signaling in LMS cells. LDE225 and Gant61 were used in this study because they are already established as potent inhibitors of SMO and GLI, respectively. Although both drugs had suppressed the LMS cells proliferation, LDE225 showed a more potent effect in decreasing of GLI nuclear expression than Gant61 treatment.

The anti-tumor effect of LDE225 observed in our model was consistent with literature for other types of cancer. For instance, in renal carcinoma cells, treatment with LDE225 showed reduced cell proliferation concomitant with lower GLI1 and GLI2 expression (28). In melanoma cells, treatment with LDE225 showed a decrease in apoptosis rate and cell proliferation, as well as an increase in cell cycle arrest. In the melanoma animal model, treatment with LDE225 inhibited GLI1 expression (29). In Hepatoma cells, the treatment suppressed cell proliferation and decreased the protein levels of GLI2 and ABCC1 transporter (30). In lung cancer, the combined treatment with LDE225 and Erlotinib (an EGFR inhibitor) showed a reduction in cell invasion, migration, colony formation, proliferation, and induced apoptosis (31). In chronic myeloid leukemia, LDE225 treatment inhibited the cell growth with GLI1 downregulation (32). Studies in LMS and other types of cancers using LDE225 demonstrated that targeting SMO is sufficient to suppress the phenotype and pathogenesis of these aggressive tumors.

Targeting GLI1 with Gant61 has been studied in other types of cancers showing beneficial effects. In breast cancer, Gant61 treatment decreased cell proliferation by reducing GLI1 and PTCH1 gene expression and inhibited GLI1 nuclear translocation (33). *In vivo* studies showed that Gant61 treatment reduced both tumor growth and GLI1 expression in rhabdomyosarcoma (34). In prostate cancer, treatment with Gant61 induced suppression of tumor growth with decreased GLI1 and PTCH1 expression (35). Our results showed that Gant61 is able to impair GLI protein expression, reduce GL1 nuclear translocation as well as exhibited an inhibitory effect on LMS cells proliferation. All those studies demonstrated the important role of GLIs in cancer development, and targeting GLIs suppressed the phenotypes of several types of neoplasms.

LMS has high recurrence and metastasis rates (36). Therefore, evaluation of the effects of SMO and GLI inhibitors in the migration process was extremely important, since this mechanism is directly involved with metastasis and progression of the disease. Regarding this, our results showed that LDE225 and Gant61 have inhibitory activity in cell migration. This inhibitory effect by HH inhibitors was consistent with studies in other types of tumors (28, 37–39). In prostate cancer, Gant61 and LDE225 treatment showed a decrease in the migration capacity of the cells (40),(41). Gant61 treatment in ovarian cancer cells showed a reduction in migration with downregulation of GLI1 activity (42). In glioblastoma cells, treatment with Gant61 suppressed migration with impairment of the expression of HH components (43).

In addition to migration, Gant61 and LDE225 have been reported to induce apoptosis. In pancreatic cancer, Gant61 induces apoptosis with downregulation of GLI expression (44). In prostate cancer, Gant61 induced apoptosis (45). In melanoma cells, LDE225 increased the percentage of apoptotic cells, inhibited cell proliferation and reduced the expression of HH pathway components (46).

Inhibition of SMO or GLI using LDE225 and Gant61 respectively blocked the HH pathway in LMS, decreasing proliferation, migration and inducing apoptosis. In addition, our results showed that the downregulation of PTCH1 in LMS indicates a possible aberrant CpG island hypermethylation of the PTCH1 gene. Activation of the HH signaling pathway can also occur due to the methylation mechanism. PTCH1 promoter region has been shown to be hypermethylated in rhabdomyosarcoma and

medulloblastoma (19) and breast cancer (20, 21). The treatment with 5'-Aza-dc in rhabdomyosarcoma and medulloblastoma showed a decrease in PTCH1 gene methylation (19). However, we did not find effects on *PTCH1* expression after 5'-Aza-dc treatment.

Interestingly, the treatment with 5'-Aza-dc in LMS regulated GLI1 expression, decrease proliferation, migration and inducing apoptosis. The mechanism in which 5'-Aza-dc regulates GLI1 expression in LMS is not understood. It may occur due to indirect regulation of GLI1 expression by cross-talk with other signalings (AKT1, TGFβ, WIP1 and HDAC), therefore activate GLI1 expression.

We explored the effect of combination treatment using 5'-Aza-dc and Gant61. The results showed a synergistic effect with those drugs. Combination treatment exhibited a more potent effect compared to single treatment in the context of inhibiting the HH pathway and affecting LMS cells proliferative and migratory behavior. The combination treatment with HH and epigenetic inhibitors has been shown to exhibit a more potent effect compared to a single treatment in other types of tumors. In liver cancer, SMO and HDAC inhibitors showed decrease cell viability, colony formation and increase apoptosis (47). In aerodigestive cancer, the combined treatment with SMO and HDAC inhibitors promote cell cycle arrest, suppress SMO and PTCH1 expression and delay tumor growth in animal model prolonging survival more than single agent alone (48). Our study using a combination treatment strategy to produce synergistic activity is one possible advance towards achieving higher cure rates in LMS.

We proposed a mechanism model of HH pathway activation in LMS based on our novel findings that 1) SMO and GLI expression are deregulated in LMS cells, 2) GLI nuclear translocation is increased in LMS cells, 3) deregulation of the epigenetic mechanism is involved in GLI1 expression, and 4) targeting HH pathway via pharmacological inhibition is able to inhibit the LMS phenotype (Figure 6 F).

Conclusion

In Summary, our studies demonstrated for the first time that HH signaling is activated in LMS cells with evidence of increased expression and nuclear translocation of GLI. We also demonstrated that impairment of HH signaling with SMO and GLI inhibitors was capable of suppressing LMS phenotype along with decreased GLI nuclear translocation. Besides, the DNMTi treatment alone or combination with GLI inhibitor had a more potent effect on the LMS malignant phenotype. All these data open new perspectives for uterine management, focusing on the development of novel non-invasive specific therapeutics for this aggressive tumor.

Abbreviations

LMS: Leiomyosarcoma; HuLM: Human leiomyoma; UTSM: Human uterine smooth muscle; HH: Hedgehog; HHIP: Hedgehog interacting protein; cDNA: complementary DNA; qRT-PCR: Quantitative real-time polymerase chain reaction; mRNA: messenger RNA; DNMT: DNA methyltransferase; 5'-Aza-dc: 5'-Aza–2'-Deoxycytidine.

Declarations

Ethics approval and consent to participate:

Not applicable

Consent for publication:

Not applicable

Availability of data and materials:

All data generated or analyzed during this study are included in this published and article and it is the Supplementary file.

Competing interests

The authors declare that they have no conflict of interest.

Funding:

This study was supported by Fundação de Amparo à Pesquisa do Estado de São Paulo (FAPESP) (FAPESP 2017/24448-1) for Natalia Garcia's scholarship. National Institutes of Health (NHI) grants RO1 HD094378; RO1 ES028615; U54 MD007602 and RO1 HD094380. None of the aforementioned funding agencies played a role in the study design, collection, analysis, interpretation of data, and writing of the manuscript.

Author Contribution:

AA, KCC, and QY contributed to the conceptual design. NG designed and conducted experiments. NG, AA and QY analyzed the data. NG wrote the draft of the manuscript. AA, KCC, ECB and QY revised the manuscript.

Acknowledgments:

Not applicable

References

1. D'Angelo E, Prat J. Uterine sarcomas: a review. Gynecologic oncology. 2010;116(1):131-9.
2. Skorstad M, Kent A, Lieng M. Uterine leiomyosarcoma - incidence, treatment, and the impact of morcellation. A nationwide cohort study. Acta obstetricia et gynecologica Scandinavica. 2016;95(9):984-90.
3. Seagle BL, Sobecki-Rausch J, Strohl AE, Shilpi A, Grace A, Shahabi S. Prognosis and treatment of uterine leiomyosarcoma: A National Cancer Database study. Gynecologic oncology. 2017;145(1):61-70.
4. Hensley ML, Blessing JA, Mannel R, Rose PG. Fixed-dose rate gemcitabine plus docetaxel as first-line therapy for metastatic uterine leiomyosarcoma: a Gynecologic Oncology Group phase II trial. Gynecologic oncology. 2008;109(3):329-34.
5. Gadducci A, Landoni F, Sartori E, Zola P, Maggino T, Lissoni A, et al. Uterine leiomyosarcoma: analysis of treatment failures and survival. Gynecologic oncology. 1996;62(1):25-32.
6. Garcia N, Bozzini N, Baiocchi G, da Cunha IW, Maciel GA, Soares Junior JM, et al. May Sonic Hedgehog proteins be markers for malignancy in uterine smooth muscle tumors? Hum Pathol. 2016;50:43-50.
7. Li X, Chen F, Zhu Q, Ding B, Zhong Q, Huang K, et al. Gli-1/PI3K/AKT/NF-kB pathway mediates resistance to radiation and is a target for reversion of responses in refractory acute myeloid leukemia cells. Oncotarget. 2016;7(22):33004-15.
8. Magistri P, Battistelli C, Strippoli R, Petrucciani N, Pellinen T, Rossi L, et al. SMO Inhibition Modulates Cellular Plasticity and Invasiveness in Colorectal Cancer. Frontiers in pharmacology. 2017;8:956.
9. Yin VT, Esmaeli B. Targeting the Hedgehog Pathway for Locally Advanced and Metastatic Basal Cell Carcinoma. Current pharmaceutical design. 2017;23(4):655-9.
10. Skoda AM, Simovic D, Karin V, Kardum V, Vranic S, Serman L. The role of the Hedgehog signaling pathway in cancer: A comprehensive review. Bosnian journal of basic medical sciences. 2018;18(1):8-20.
11. Carballo GB, Honorato JR, de Lopes GPF, Spohr T. A highlight on Sonic hedgehog pathway. Cell communication and signaling : CCS. 2018;16(1):11.
12. Zeng X, Ju D. Hedgehog Signaling Pathway and Autophagy in Cancer. International journal of molecular sciences. 2018;19(8).
13. Kasper M, Regl G, Frischauf AM, Aberger F. GLI transcription factors: mediators of oncogenic Hedgehog signalling. Eur J Cancer. 2006;42(4):437-45.
14. Duan ZH, Wang HC, Zhao DM, Ji XX, Song M, Yang XJ, et al. Cooperatively transcriptional and epigenetic regulation of sonic hedgehog overexpression drives malignant potential of breast cancer. Cancer science. 2015;106(8):1084-91.
15. Cui W, Wang LH, Wen YY, Song M, Li BL, Chen XL, et al. Expression and regulation mechanisms of Sonic Hedgehog in breast cancer. Cancer science. 2010;101(4):927-33.

16. Loh M, Liem N, Vaithilingam A, Lim PL, Sapari NS, Elahi E, et al. DNA methylation subgroups and the CpG island methylator phenotype in gastric cancer: a comprehensive profiling approach. BMC gastroenterology. 2014;14:55.
17. Lin EH, Kao YR, Lin CA, Kuo TY, Yang SP, Hsu CF, et al. Hedgehog pathway maintains cell survival under stress conditions, and drives drug resistance in lung adenocarcinoma. Oncotarget. 2016;7(17):24179-93.
18. Tada M, Kanai F, Tanaka Y, Tateishi K, Ohta M, Asaoka Y, et al. Down-regulation of hedgehog-interacting protein through genetic and epigenetic alterations in human hepatocellular carcinoma. Clinical cancer research : an official journal of the American Association for Cancer Research. 2008;14(12):3768-76.
19. Ecke I, Petry F, Rosenberger A, Tauber S, Monkemeyer S, Hess I, et al. Antitumor effects of a combined 5-aza-2'deoxycytidine and valproic acid treatment on rhabdomyosarcoma and medulloblastoma in Ptch mutant mice. Cancer research. 2009;69(3):887-95.
20. Wolf I, Bose S, Desmond JC, Lin BT, Williamson EA, Karlan BY, et al. Unmasking of epigenetically silenced genes reveals DNA promoter methylation and reduced expression of PTCH in breast cancer. Breast Cancer Res Treat. 2007;105(2):139-55.
21. Sinha S, Singh RK, Alam N, Roy A, Roychoudhury S, Panda CK. Alterations in candidate genes PHF2, FANCC, PTCH1 and XPA at chromosomal 9q22.3 region: pathological significance in early- and late-onset breast carcinoma. Molecular cancer. 2008;7:84.
22. Diede SJ, Guenthoer J, Geng LN, Mahoney SE, Marotta M, Olson JM, et al. DNA methylation of developmental genes in pediatric medulloblastomas identified by denaturation analysis of methylation differences. Proceedings of the National Academy of Sciences of the United States of America. 2010;107(1):234-9.
23. Brinkhuizen T, van den Hurk K, Winnepenninckx VJ, de Hoon JP, van Marion AM, Veeck J, et al. Epigenetic changes in Basal Cell Carcinoma affect SHH and WNT signaling components. PloS one. 2012;7(12):e51710.
24. Zuo Y, Song Y, Zhang M, Xu Z, Qian X. Role of PTCH1 gene methylation in gastric carcinogenesis. Oncol Lett. 2014;8(2):679-82.
25. Chakraborty C, Dutta S, Mukherjee N, Samadder S, Roychowdhury A, Roy A, et al. Inactivation of PTCH1 is associated with the development of cervical carcinoma: clinical and prognostic implication. Tumour biology : the journal of the International Society for Oncodevelopmental Biology and Medicine. 2015;36(2):1143-54.
26. Zuo Y, Song Y. Detection and analysis of the methylation status of PTCH1 gene involved in the hedgehog signaling pathway in a human gastric cancer cell line. Experimental and therapeutic medicine. 2013;6(6):1365-8.
27. Liang CC, Park AY, Guan JL. In vitro scratch assay: a convenient and inexpensive method for analysis of cell migration in vitro. Nature protocols. 2007;2(2):329-33.

28. D'Amato C, Rosa R, Marciano R, D'Amato V, Formisano L, Nappi L, et al. Inhibition of Hedgehog signalling by NVP-LDE225 (Erismodegib) interferes with growth and invasion of human renal cell carcinoma cells. Br J Cancer. 2014;111(6):1168-79.
29. Jalili A, Mertz KD, Romanov J, Wagner C, Kalthoff F, Stuetz A, et al. NVP-LDE225, a potent and selective SMOOTHENED antagonist reduces melanoma growth in vitro and in vivo. PloS one. 2013;8(7):e69064.
30. Ding J, Zhou XT, Zou HY, Wu J. Hedgehog signaling pathway affects the sensitivity of hepatoma cells to drug therapy through the ABCC1 transporter. Laboratory investigation; a journal of technical methods and pathology. 2017;97(7):819-32.
31. Della Corte CM, Bellevicine C, Vicidomini G, Vitagliano D, Malapelle U, Accardo M, et al. SMO Gene Amplification and Activation of the Hedgehog Pathway as Novel Mechanisms of Resistance to Anti-Epidermal Growth Factor Receptor Drugs in Human Lung Cancer. Clinical cancer research : an official journal of the American Association for Cancer Research. 2015;21(20):4686-97.
32. Irvine DA, Zhang B, Kinstrie R, Tarafdar A, Morrison H, Campbell VL, et al. Deregulated hedgehog pathway signaling is inhibited by the smoothened antagonist LDE225 (Sonidegib) in chronic phase chronic myeloid leukaemia. Sci Rep. 2016;6:25476.
33. Benvenuto M, Masuelli L, De Smaele E, Fantini M, Mattera R, Cucchi D, et al. In vitro and in vivo inhibition of breast cancer cell growth by targeting the Hedgehog/GLI pathway with SMO (GDC-0449) or GLI (GANT-61) inhibitors. Oncotarget. 2016;7(8):9250-70.
34. Srivastava RK, Kaylani SZ, Edrees N, Li C, Talwelkar SS, Xu J, et al. GLI inhibitor GANT-61 diminishes embryonal and alveolar rhabdomyosarcoma growth by inhibiting Shh/AKT-mTOR axis. Oncotarget. 2014;5(23):12151-65.
35. Lauth M, Bergstrom A, Shimokawa T, Toftgard R. Inhibition of GLI-mediated transcription and tumor cell growth by small-molecule antagonists. Proceedings of the National Academy of Sciences of the United States of America. 2007;104(20):8455-60.
36. Cui RR, Wright JD, Hou JY. Uterine leiomyosarcoma: a review of recent advances in molecular biology, clinical management and outcome. Bjog. 2017;124(7):1028-37.
37. Chen Q, Xu R, Zeng C, Lu Q, Huang D, Shi C, et al. Down-regulation of Gli transcription factor leads to the inhibition of migration and invasion of ovarian cancer cells via integrin beta4-mediated FAK signaling. PLoS One. 2014;9(2):e88386.
38. Habib JG, O'Shaughnessy JA. The hedgehog pathway in triple-negative breast cancer. Cancer Med. 2016;5(10):2989-3006.
39. Mechlin CW, Tanner MJ, Chen M, Buttyan R, Levin RM, Mian BM. Gli2 expression and human bladder transitional carcinoma cell invasiveness. J Urol. 2010;184(1):344-51.
40. Nanta R, Shrivastava A, Sharma J, Shankar S, Srivastava RK. Inhibition of sonic hedgehog and PI3K/Akt/mTOR pathways cooperate in suppressing survival, self-renewal and tumorigenic potential of glioblastoma-initiating cells. Mol Cell Biochem. 2019;454(1-2):11-23.

41. Nanta R, Kumar D, Meeker D, Rodova M, Van Veldhuizen PJ, Shankar S, et al. NVP-LDE-225 (Erismodegib) inhibits epithelial-mesenchymal transition and human prostate cancer stem cell growth in NOD/SCID IL2Rgamma null mice by regulating Bmi-1 and microRNA-128. Oncogenesis. 2013;2:e42.
42. Liu Y, Gao S, Zhu J, Zheng Y, Zhang H, Sun H. Dihydroartemisinin induces apoptosis and inhibits proliferation, migration, and invasion in epithelial ovarian cancer via inhibition of the hedgehog signaling pathway. Cancer Med. 2018;7(11):5704-15.
43. Sun W, Li L, Du Z, Quan Z, Yuan M, Cheng H, et al. Combination of phospholipase Cepsilon knockdown with GANT61 sensitizes castrationresistant prostate cancer cells to enzalutamide by suppressing the androgen receptor signaling pathway. Oncol Rep. 2019;41(5):2689-702.
44. Ghanbari A, Cheraghzadeh Z, Mahmoudi R, Zibara K, Hosseini E. GLI inhibitors overcome Erlotinib resistance in human pancreatic cancer cells by modulating E-cadherin. J Chemother. 2019;31(3):141-9.
45. Tong W, Qiu L, Qi M, Liu J, Hu K, Lin W, et al. GANT-61 and GDC-0449 induce apoptosis of prostate cancer stem cells through a GLI-dependent mechanism. J Cell Biochem. 2018;119(4):3641-52.
46. O'Reilly KE, de Miera EV, Segura MF, Friedman E, Poliseno L, Han SW, et al. Hedgehog pathway blockade inhibits melanoma cell growth in vitro and in vivo. Pharmaceuticals (Basel). 2013;6(11):1429-50.
47. Li J, Cai H, Li H, Liu Y, Wang Y, Shi Y, et al. Combined inhibition of sonic Hedgehog signaling and histone deacetylase is an effective treatment for liver cancer. Oncology reports. 2019;41(3):1991-7.
48. Chun SG, Park H, Pandita RK, Horikoshi N, Pandita TK, Schwartz DL, et al. Targeted inhibition of histone deacetylases and hedgehog signaling suppress tumor growth and homologous recombination in aerodigestive cancers. American journal of cancer research. 2015;5(4):1337-52.
49. Ming J, Sun B, Li Z, Lin L, Meng X, Han B, et al. Aspirin inhibits the SHH/GLI1 signaling pathway and sensitizes malignant glioma cells to temozolomide therapy. Aging (Albany NY). 2017;9(4):1233-47.
50. Kawabata N, Ijiri K, Ishidou Y, Yamamoto T, Nagao H, Nagano S, et al. Pharmacological inhibition of the Hedgehog pathway prevents human rhabdomyosarcoma cell growth. Int J Oncol. 2011;39(4):899-906.
51. Wei F, Zhou J, Wei X, Zhang J, Fleming BC, Terek R, et al. Activation of Indian hedgehog promotes chondrocyte hypertrophy and upregulation of MMP-13 in human osteoarthritic cartilage. Osteoarthritis Cartilage. 2012;20(7):755-63.
52. Magistri P, Battistelli C, Strippoli R, Petrucciani N, Pellinen T, Rossi L, et al. SMO Inhibition Modulates Cellular Plasticity and Invasiveness in Colorectal Cancer. Front Pharmacol. 2017;8:956.
53. Zhang Z, Zou Y, Liang M, Chen Y, Luo Y, Yang B, et al. Suppressor of fused (Sufu) promotes epithelial-mesenchymal transition (EMT) in cervical squamous cell carcinoma. Oncotarget. 2017;8(69):114226-38.
54. Xu L, Liu H, Yan Z, Sun Z, Luo S, Lu Q. Inhibition of the Hedgehog signaling pathway suppresses cell proliferation by regulating the Gli2/miR-124/AURKA axis in human glioma cells. Int J Oncol.

2017;50(5):1868-78.

55. Gonnissen A, Isebaert S, McKee CM, Dok R, Haustermans K, Muschel RJ. The hedgehog inhibitor GANT61 sensitizes prostate cancer cells to ionizing radiation both in vitro and in vivo. Oncotarget. 2016;7(51):84286-98.
56. Teng Y, Yu X, Yuan H, Guo L, Jiang W, Lu SH. DNMT1 ablation suppresses tumorigenesis by inhibiting the self-renewal of esophageal cancer stem cells. Oncotarget. 2018;9(27):18896-907.
57. Zhao Z, Wu Q, Cheng J, Qiu X, Zhang J, Fan H. Depletion of DNMT3A suppressed cell proliferation and restored PTEN in hepatocellular carcinoma cell. J Biomed Biotechnol. 2010;2010:737535.
58. Liao J, Karnik R, Gu H, Ziller MJ, Clement K, Tsankov AM, et al. Targeted disruption of DNMT1, DNMT3A and DNMT3B in human embryonic stem cells. Nat Genet. 2015;47(5):469-78.
59. Paschke L, Jopek K, Szyszka M, Tyczewska M, Ziolkowska A, Rucinski M, et al. ZFP91: A Noncanonical NF-kappaB Signaling Pathway Regulator with Oncogenic Properties Is Overexpressed in Prostate Cancer. Biomed Res Int. 2016;2016:6963582.

Figures

Figure 1

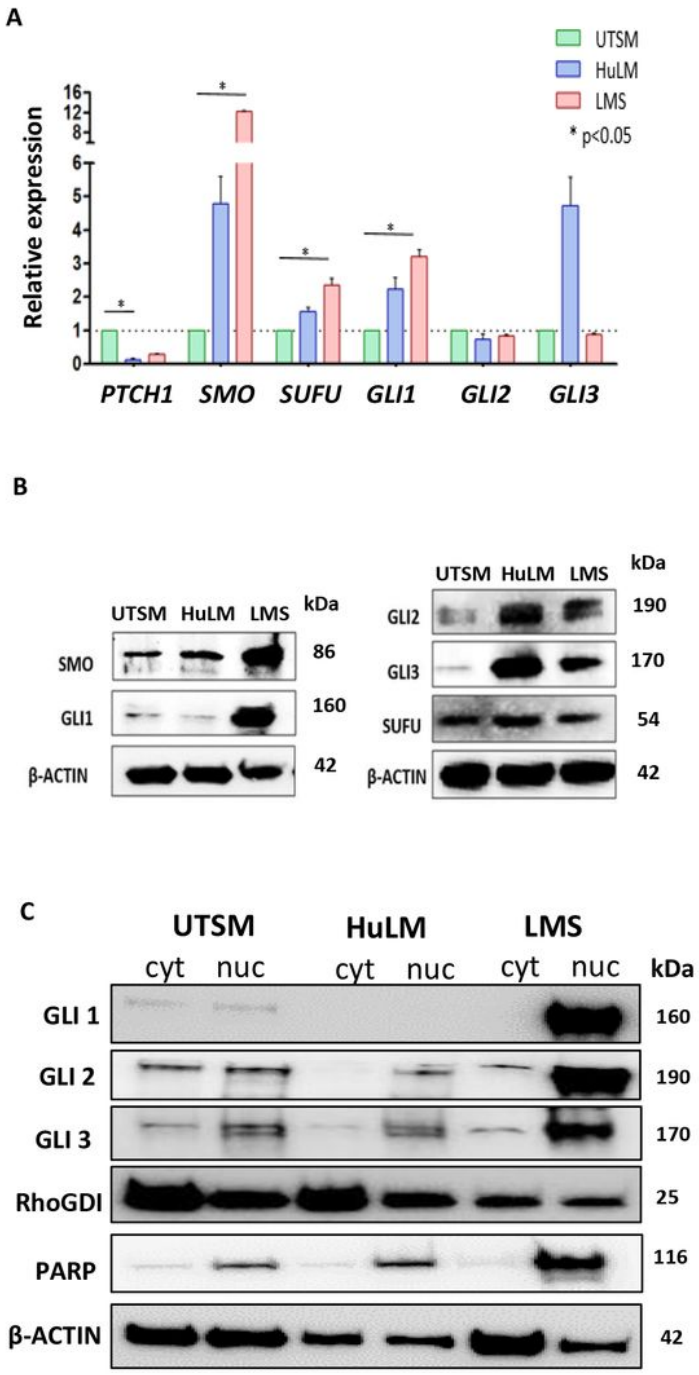

Figure 1

Basal HH signaling components gene and protein expression in UTSM, HuLM, and LMS cell lines. A: mRNA expression levels of PTCH1, SMO, SUFU, GLI1, GLI2, and GLI3 quantified by qRT-PCR. Relative expression values were obtained after reference and endogenous control normalization. B: Protein expression of SMO, SUFU, GLI1, GLI2 and GLI3 in the left panel. C: Protein expression of GLI1, 2, and 3 in both cytoplasm and nucleus compartment of the cells. * p<0.05

Figure 2

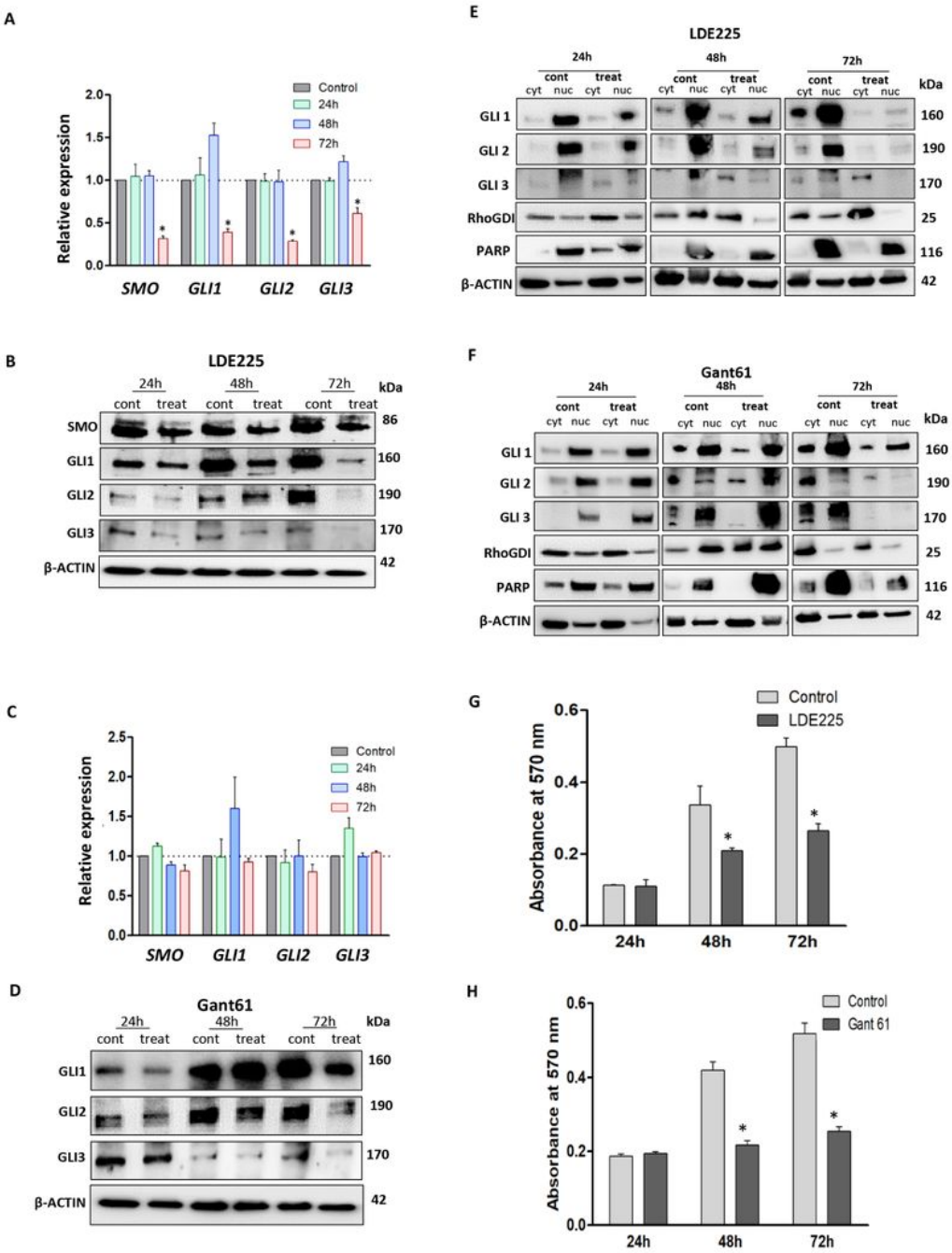

Figure 2

Treatment with HH inhibitors decrease transcript and protein levels and reduced LMS cell proliferation. A: RNA expression of HH components (SMO, GLI1, GLI2, and GLI3) using LDE225, B: Western blot images showing protein expression profile of SMO, GLI1, GLI2 and GLI3 after SMO inhibition (LDE225). C: RNA expression of HH components after GLI inhibition. D: Protein expression of GLI1, GLI2, and GLI3 after Gant61 treatment. E and F: GLIs proteins expression in the cytoplasm and nucleus compartments after

72 hours of treatment with LDE225 and Gant61, respectively. G and H: MTT assays comparing the proliferation profile of LMS cells after treatments at different time points (24, 48 and 72 hours). * p<0.05

Figure 3

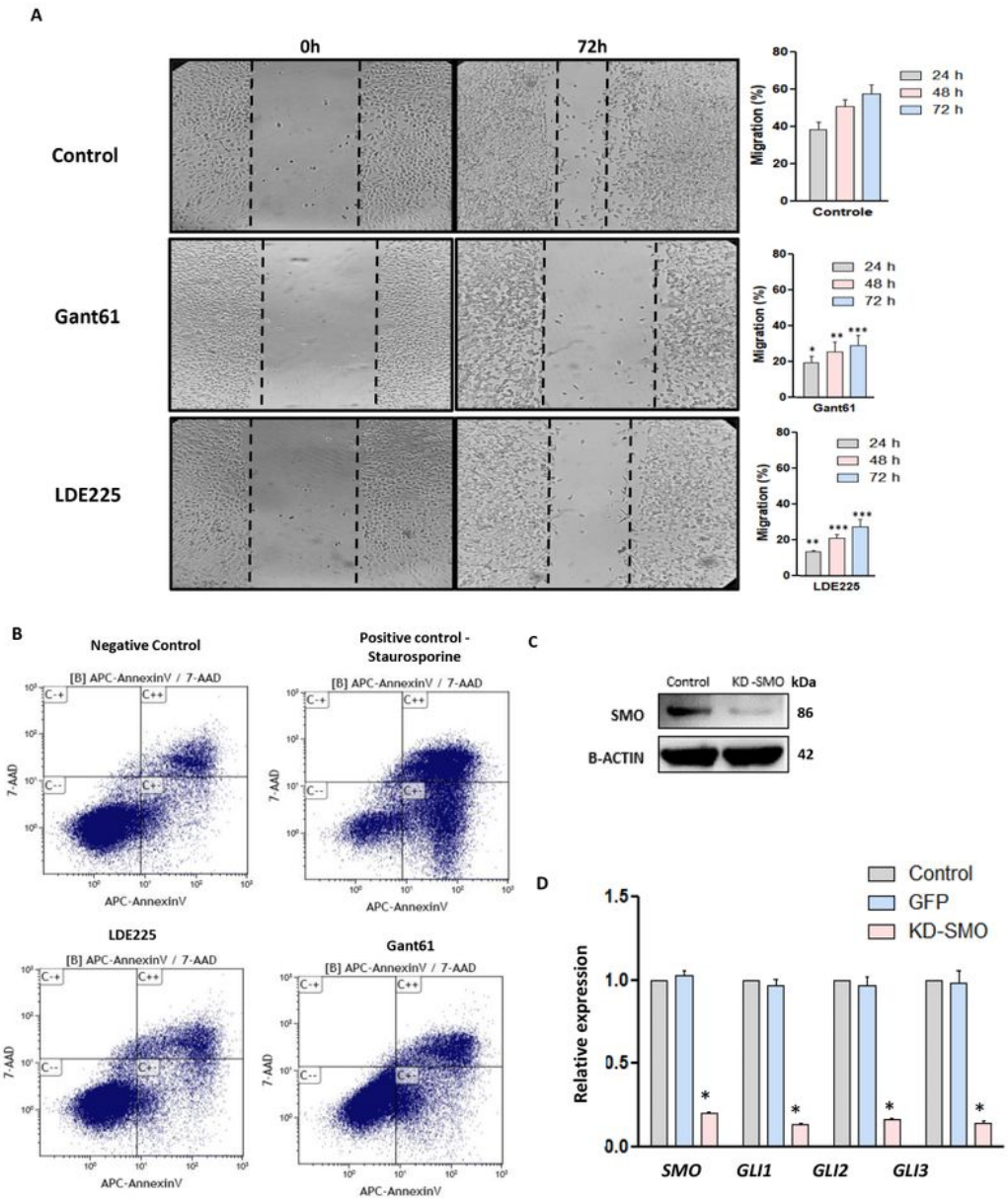

Figure 3

Effect of HH inhibitors on migration and apoptosis in LMS cells and knockdown of SMO. A: Would healing assay (20x), the bar chart showing quantitative analysis of cell migration after 72h of treatment comparing to the control (no treated). B: Apoptosis rates of LMS cell (annexin V assay) after 72 hours

with SMO or GLI inhibitors. Staurosporine treatment was used as a positive control (24 hours). C: SMO protein expression after SMO gene knockdown. D: RNA expression of HH components after SMO gene knockdown. * p<0.05, ** p<0.01, *** p<0.001

Figure 4

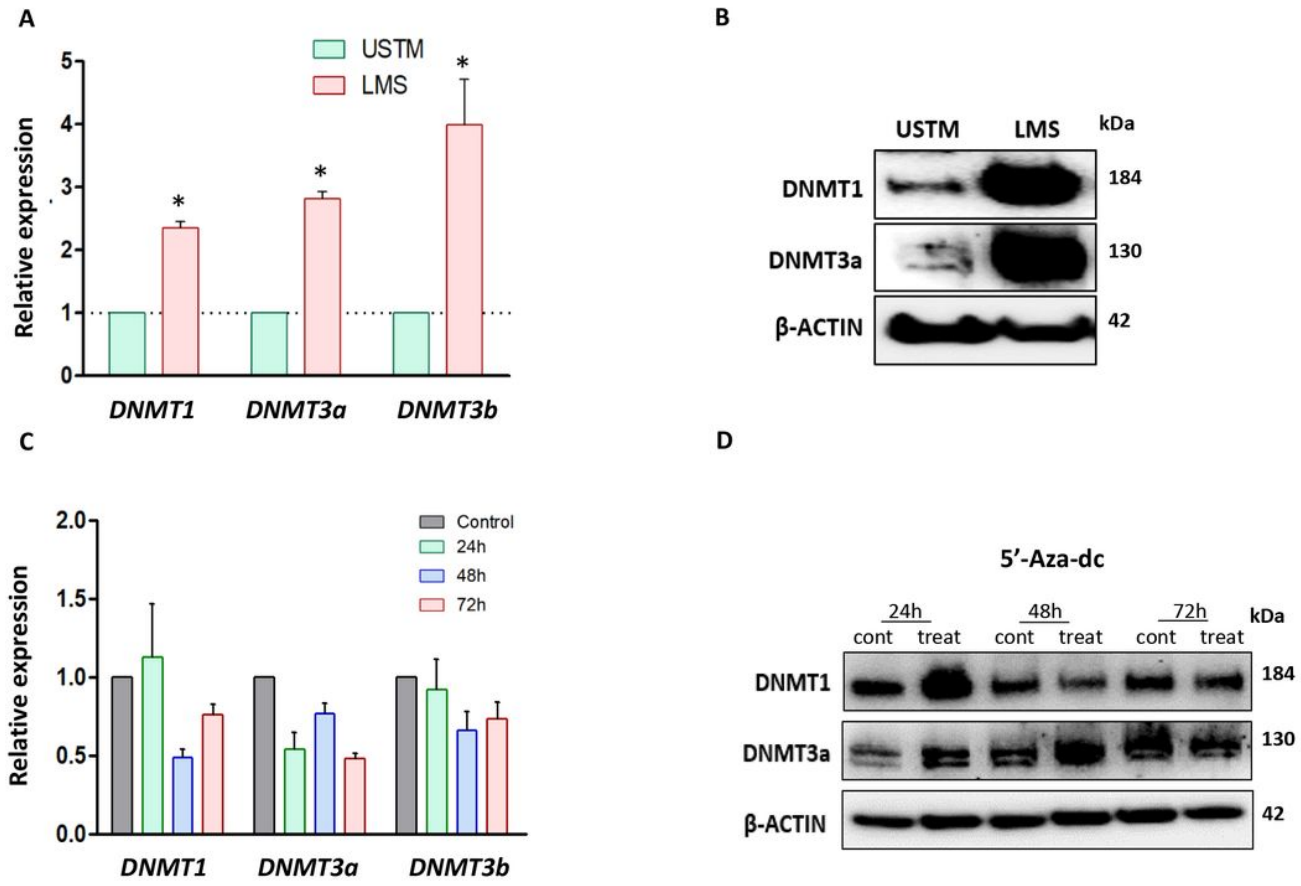

Figure 4

DNMTs expression levels in LMS cells, and the effects of DNMT inhibitor. A: mRNA levels of DNMTs (DNMT1, DNMT3a, and DNMT3b) in UTSM and LMS. B: Protein expression of DNMT1 and DNMT3a in UTSM and LMS by Western Blot. C: RNA expression of DNMT1, DNMT3a, and DNMT3b in response to 5'-Aza-dc treatment for 72 h. D: Protein expression of DNMTs (DNMT1 and DNMT3a) in response to 5-Aza-dc treatment for 72 h, and quantification analysis of DNMTs protein. * p<0.05

Figure 5

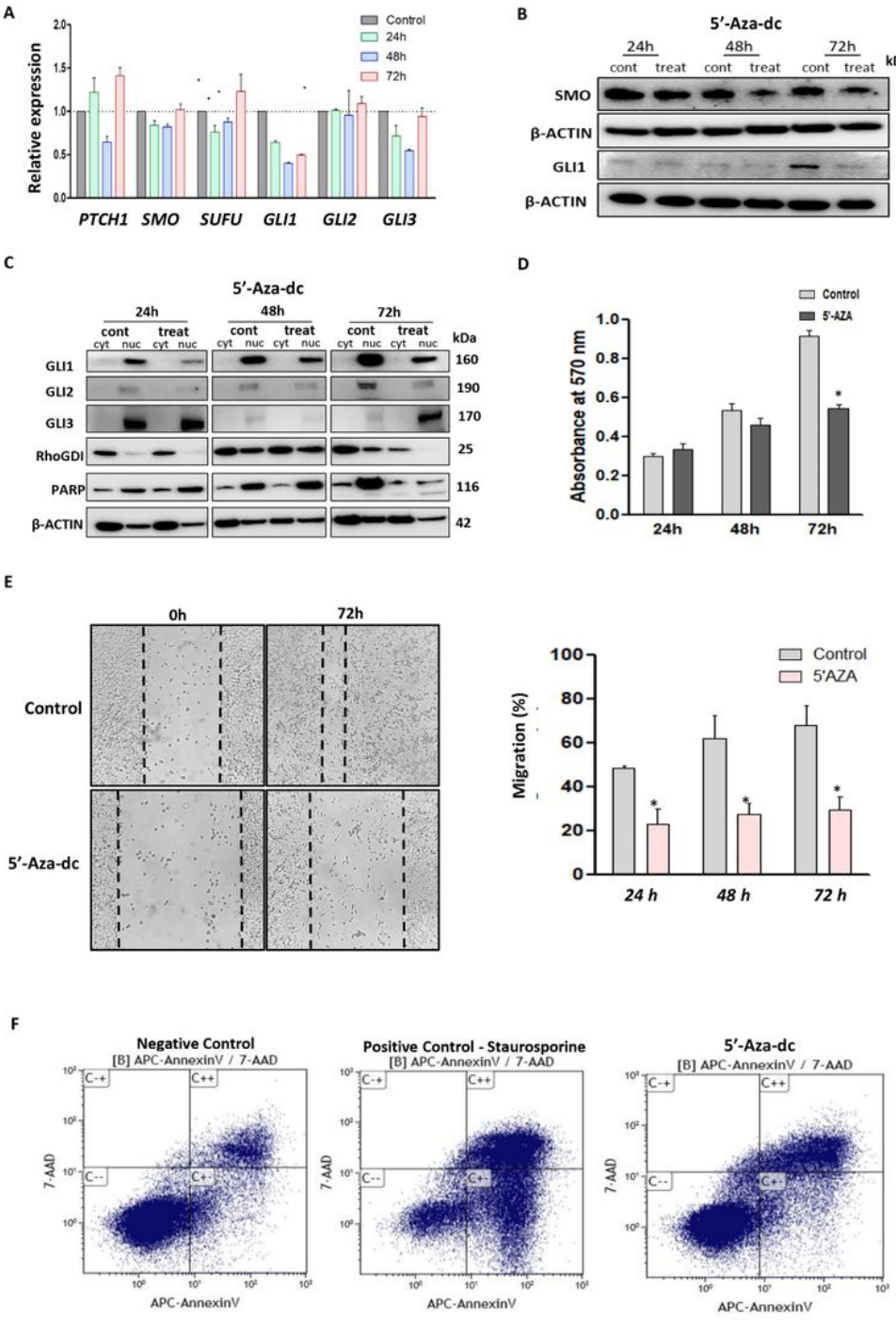

Figure 5

DNMTs inhibition and its effects on GLI1 expression, cell proliferation, cell migration and apoptosis induction. A: PTCH1, SMO, SUFU, GLI1, GLI2 and GLI3 expression after 5'-Aza-dc cell treatment compared to control (no treated cells). B: Protein expression of SMO and GLI1 with or without 5'-Aza-dc treatment. C: GLIs protein expression in cytoplasm and nuclear cell compartment, after 72 hours of 5'-Aza-dc treatment. D: MTT assay in the presence or absence of 5'-Aza-dc for 72 hours. E: Wound healing assay

(20x) for cell migration measuring after 72 h of 5'Aza treatment, and quantification analysis of percentage of migration. F: Apoptosis assay using annexin V stain after 72 h of 5'-Aza-dc treatment. Staurosporine treatment for 24 h was used as a positive control. * p<0.05, ** p<0.01, *** p<0.001

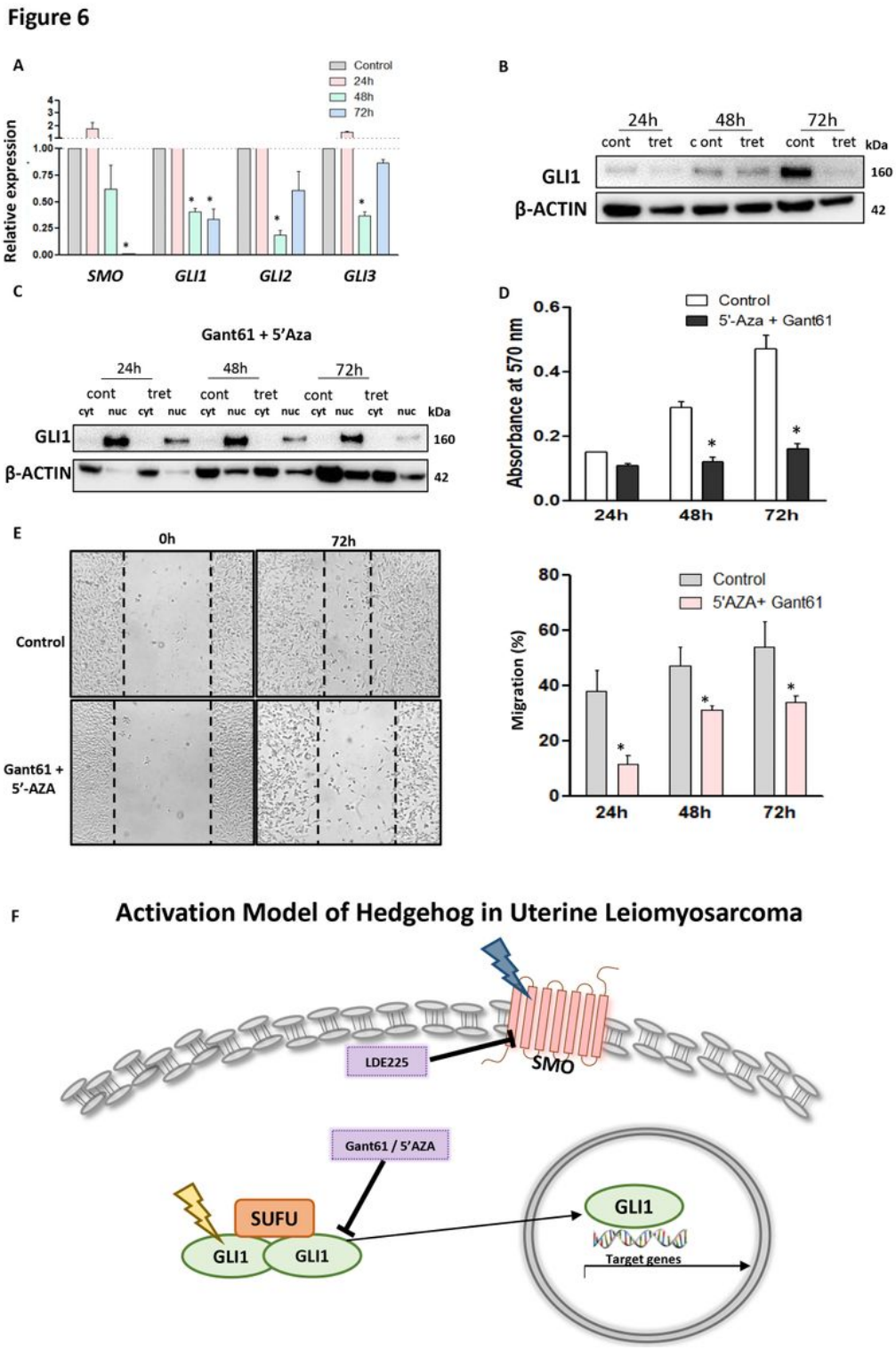

Figure 6

Effects of combination treatment with 5'-Aza-dc and Gant61 on HH signaling in LMS cells. A: RNA expression of SMO, GLI1, GLI2, and GLI3 with combination treatment or without treatment. B: GLI1 protein

expression in the presence or absence of the combination treatment. C: GLI1 protein expression in the cytoplasm and nuclear compartment. D: Measurement of cell proliferation using MTT assay. E: Wound healing assay after 72 h of the combination treatment and quantification analysis of the percentage of migration. * $p<0.05$, ** $p<0.01$, *** $p<0.001$. F: Proposed model of HH signaling pathway activation in uterine LMS cells. The expression of SMO and GLI is deregulated and GLI nuclear translocation is increased, and targeting these molecules were able to inhibit the LMS phenotype. We also proposed that the epigenetic mechanism is involved in the hyper-regulation of GLI1 expression. The deregulation of SMO and GLI1 are represented in yellow and blue

Supplementary Files

This is a list of supplementary files associated with this preprint. Click to download.

- Additionalfile2.pdf
- Additionalfile5.pdf
- Additionalfile4.pdf
- Additionalfile6.pdf
- Additionalfile1.pdf
- Additionalfile7.pdf
- Additionalfile3.pdf